SensHB.Q: A Cost-Effective Force-Sensitive Handlebar to Control Omnidirectional Robots and Wheelchairs

Journal of Field Robotics

WILEY

RESEARCH ARTICLE OPEN ACCESS

SensHB.Q: A Cost-Effective Force-Sensitive Handlebar to Control Omnidirectional Robots and Wheelchairs

Luigi Tagliavini | Giuseppe Quaglia

Department of Mechanical and Aerospace Engineering, Politecnico di Torino, Torino, Italy

Correspondence: Luigi Tagliavini (luigi.tagliavini@polito.it)

Received: 22 July 2024 | **Revised:** 21 July 2025 | **Accepted:** 27 September 2025

Keywords: drive interface | force-sensitive system | motorized systems | omnidirectional robots | omnidirectional wheelchairs | six-bar linkage | uniaxial load cells

ABSTRACT

This paper details the design and development of SensHB.Q, a force-sensitive handlebar intended for caregivers driving electric-powered wheelchairs, particularly those with omnidirectional mobility. The same interface can also be used in the future to operate other omnidirectional motorized systems, such as mobile robots, hospital beds, and industrial trolleys. The primary objective was to develop an intuitive, cost-effective device. To achieve this, the interface mimics the way we naturally interact with objects by applying forces and torques to achieve desired movements. SensHB.Q measures the forces and torques applied by the driver and converts them into commands for the motorized system. The idea is that the driver applies small forces and torques, and the motorized platform then takes care of the traction forces needed to perform the desired motion. In terms of cost-effectiveness, SensHB.Q uses a mechanism that only employs uniaxial load cells to measure the forces applied by the driver, thus avoiding the need for costly multiaxial load cells. This paper first presents the concept of SensHB, followed by a discussion of its functional and executive design. Second, the study elaborates on the electronic control unit of the device and presents experimental tests comparing the force/torque measurements of SensHB.Q with those of an off-the-shelf, six-axis force/torque sensor. Finally, SensHB.Q is integrated and tested on the omnidirectional motorized wheelchair MoviWE.Q, which was developed at Politecnico di Torino. These preliminary tests, which are performed with a limited number of participants, are used to test whether it is possible to drive an omnidirectional motorized system using the developed force-sensitive interface.

1 | Introduction

Technological advancements in recent decades have facilitated the proliferation of various motorized systems, including mobile robots (Bruzzone and Quaglia 2012), motorized carts, lifts, and wheelchairs (Ding and Cooper 2005). These systems are designed to assist individuals in performing activities that would otherwise be physically demanding, tiring, or even unachievable. Every motorized system requires a suitable control interface that enables drivers to operate the device effectively. This interface must satisfy several key requirements, including:

- *Drivability:* The interface must enable drivers to have complete control over the motorized device.
- *Ergonomics:* The interface should be designed for comfort, minimizing issues related to incorrect posture or discomfort during operation.
- *Ease of Use:* Ideally, the interface should be intuitive and straightforward to operate, requiring little to no specific training for drivers.
- *Safety:* The interface must distinguish between intentional driver commands and accidental inputs, ensuring safe operation of the motorized device.

The most commonly used interface for controlling motorized mobile devices is the joystick. This peripheral device typically consists of a lever that can be tilted from its neutral position,

which is maintained by a return spring. The lever's tilt can occur along one or more axes where angular position transducers are installed to measure its angles of tilt. From a functional perspective, the joystick generates reference signals based on the rotation of the lever. These control interfaces facilitate the generation of reference signals in a straightforward and reliable manner. Joysticks find widespread application in managing virtual environments (such as gaming or simulators) (Lapointe and Vinson 2002; Marchal et al. 2011), in remote controller for mobile devices (including drones, search and rescue robots, lifting systems, etc.) (Yang et al. 2023; Kim and Chang 2022; Nosirov et al. 2020), and electric-powered wheelchairs (EPWs) (J. H. Choi et al. 2019; Shibata et al. 2015). Specifically, lever joysticks are well-suited for controlling motorized devices where the joystick's base remains fixed relative to the driver. This is because accurately controlling the angular position of a lever becomes challenging when the base of the joystick moves relative to the driver.

For these types of applications, control interfaces based on measuring the forces exerted by the operator on the drive interface have been developed to address challenges posed by traditional joystick interfaces. These interfaces typically consist of handles equipped with force sensors positioned between the driver's grasp and the mobile device. This setup enables the measurement of forces and torques applied by the driver, which are then converted into reference signals for controlling the motorized system. The use of force-sensitive handlebars for smart-walkers and motorized wheelchair control has been studied previously by Alwan et al. (2007) and Trujillo-León et al. (2018). Alwan et al. (2007) investigated a motorized walker equipped with two handles, each featuring a six-axis force sensor to measure driver-applied forces. Trujillo-León et al. (2017, 2018) adopted tactile sensor arrays to measure the contact pressures exchanged between the operator's hands and the handle. Patent literature on medical beds (Blanchard et al. 2013) and industrial robotic arms (Murakami 2019) features these kinds of interfaces.

Existing force-sensitive interfaces have two main limitations regarding omnidirectional motorized system control: they rely on costly six-axis force-torque sensors (Alwan et al. 2007), or they are more cost-effective, but they can only be used to control two degrees-of-freedom systems, such as differential-drive wheelchairs or walkers (Trujillo-León et al. 2017; Martins et al. 2014; Cortes et al. 2008; Shi et al. 2010). While the former class is too expensive to be economically sustainable for the end-users, the latter is unsuitable for omnidirectional motion control.

Given the current state of research in this field, the authors believe that the literature on controlling omnidirectional mobile systems is not yet fully developed and suggests that improvements could enhance the cost-effectiveness of existing solutions. In fact, cost-effectiveness is crucial for technologies intended for everyday use. Six-axis force/torque sensors adopted in previous studies are notably expensive, in the range of 5000€ to 12,000€ considering brand, like, BOTA SYTEMS, Kistler, and Futek. Therefore, the main contribution of this study is the development of a cost-effective force-sensitive handlebar suitable for controlling omnidirectional motorized systems, that is, those mobile systems that can move in any direction in the plane of motion. These platforms are also known as holonomic mobile systems since the controllable degrees-of-freedom match the total degrees of freedom (in this case, this equals three).

The main advantage of omnidirectional mobility, compared with differential steering, skid-steering, or car-like locomotion, is the improved capability at navigating in narrow spaces and environments with lots of obstacles, like, indoor environments (e.g., houses, offices, public buildings, and school rooms). This can help people who move with wheelchairs to access indoor environments more easily. Moreover, improved mobility with lateral motion can also help adjust the final position of the wheelchair in cases, such as table approaching, elevator, and bathroom navigation. Omnidirectional mobile platforms are also adopted in other fields of applications, such as in industrial transportation systems and mobile robotics (J. Choi 2025; Neaz et al. 2023; Taheri and Zhao 2020; Tagliavini et al. 2022).

This paper presents the concept of SensHB in Section 2, the functional and executive design in Sections 3 and 4. Then, the study details the electronic control unit of the interface in Section 5, and presents, in Section 6, experimental tests to compare the sensorized-handlebar's force/torque measurements with a commercial six-axis force/torque sensor, the SensOne by BOTA SYSTEMS. Finally, a case study for the sensorized handlebar is presented in Section 7, where SensHB.Q is used to control the omnidirectional motorized wheelchair MoviWE.Q, developed at Politecnico di Torino (Tagliavini and Quaglia 2023). These preliminary tests, which are performed with a limited number of participants, aim to test the feasibility of driving an omnidirectional motorized system using the SensHB.Q. During the tests, the participants' perceived usability was recoded using NASA's Raw Task Load Index (RTLX) scales.

The experimental tests in this paper focus specifically on the application of SensHB.Q to omnidirectional EPWs. Nevertheless, the adoption of SensHB.Q in other application fields is considered straightforward, in the same way that three-dimensional (3D) joysticks are used to control mobile systems across various domains. With this concept in mind, the design of SensHB.Q has been developed with general omnidirectional motorized systems in consideration.

Finally, it is worth noting that a patent is pending on the idea behind SensHB.Q. Title: Sensorized handlebar for motorized systems, authors: Giuseppe Quaglia and Luigi Tagliavini, with a priority date of 27/02/2024 and a priority number of 102024000004177.

2 | Requirements and Concept Design

To design a new control interface for omnidirectional motorized systems, all the requirements presented at the beginning of Section 1 (drivability, ergonomics, ease of use, and safety) must be considered. Moreover, for omnidirectional mobile systems, at least three control signals must be generated. Finally, cost-effectiveness is paramount for the technology to be applied in practical applications.

To improve the intuitiveness of the device, force/torque inputs are selected for the drive interface to mimic the way we move objects around, that is, we apply forces and torques according to the desired motion we want to obtain. Therefore, the device must be able to sense the driver's forces and torques. For this reason, the device is referred to as a sensorized handlebar or force-sensitive handlebar in this paper. To measure the driver's applied wrench on the handlebar, the device must have force/torque sensors. The most straightforward solution is to use a six-axis force/torque sensor interposed between the handlebar and the motorized system, considering only the wrench components of interest. Unfortunately, this solution is not compatible with the requirement for cost-effectiveness, since six-axis force/torque sensors are very expensive. To limit the costs, the device is designed to adopt only uniaxial load cells that are easier to find in the market and more affordable. To measure only a subset of the six components of the input wrench, the device is conceived as an isostatic structure based on a mechanism with the same number of degrees of freedom as the system to be controlled. The degrees of freedom of the mechanism are aligned with the direction of the selected force/torque inputs. Then, uniaxial load cells are mounted to isostatically constrain this mechanism. Thus, the selected components of the input wrench are measured through the load cells, while all the other components are transmitted to the frame of the mechanism. Finally, the device should have a safety feature to avoid accidental impacts with the handlebar to produce movements of the motorized system. In other words, this safety feature aims to distinguish if the input forces are related to the driver's intention. A possible solution is to install proximity/contact sensors, like, capacitive sensors, inside the ergonomic handles. These sensors can be used as switches to turn on the handlebar if the caregiver correctly holds the handlebar.

Given these premises, let us consider the case where the drive interface is adopted to control the motion of omnidirectional motorized platforms, that is, platforms in which the locomotion system can control independently the linear velocity vector and yaw angular velocity. For what concerns this study, the locomotion system can either be swerve-drive based, mecanum-wheel based, omni-wheel based, or any other locomotion system that can provide the platform with omnidirectional mobility. In this case, the two force components F_x and F_y on the plane parallel to the plane of motion (the XY-plane of the $\{h\}$ frame in Figure 1) and the torque M_z around the vertical axis perpendicular to the plane of motion (the Z-axis of the $\{h\}$ frame in Figure 1) are selected as inputs (purple vectors in Figure 1). This is done to improve the intuitiveness of the device in controlling the motorized systems. In particular, Figure 1 shows two application examples: in (a), the drive interface is installed on a swerve-drive-based omnidirectional wheelchair called MoviWE.Q (Tagliavini and Quaglia 2023), while in (b), the drive interface is used to control an omnidirectional motorized industrial cart for heavy transportation.

As previously stated, the mechanism should have the same number of degrees of freedom as the system to be controlled, in this case, three. The degrees of freedom of the mechanism are aligned with the direction of the selected force/torque inputs. Therefore, without the load cells, the mechanism should leave the handlebar free to translate on the XY-plane of the h frame and rotate around the vertical Z-axis of the h frame. Then, uniaxial load cells are mounted to isostatically constrain the mechanism. In this way, only the components of interest are measured by the load cells, while the other three components of the wrench are transmitted to the structure of the mechanism. The concept of the device is summarized in Figure 2.

3 | Functional Design

This section presents the functional design of SensHB, with a particular focus on the planar mechanism and load cell layout. In Figure 3, some of the mechanisms that had been considered during the functional design of the device mechanism are depicted.

The first and most straightforward solution, shown in Figure 3a, consists of a handlebar connected to the frame of the motorized

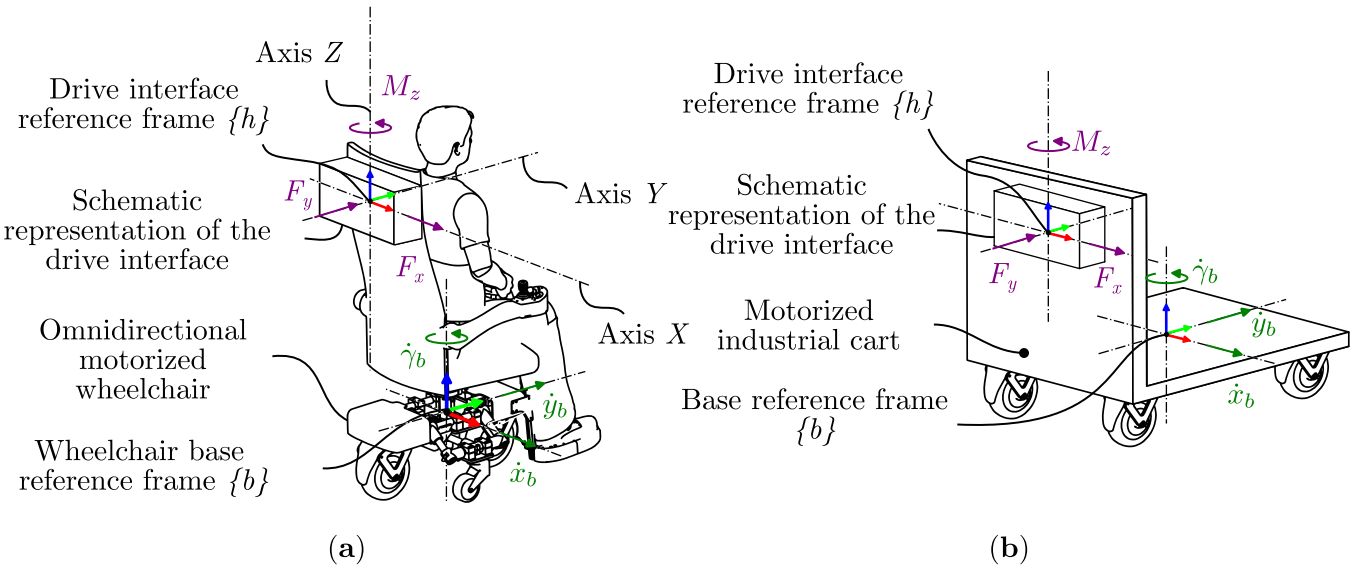

FIGURE 1 | Concept representation of the drive interface, inputs, and reference frames definition. Application examples: (a) installed on an omnidirectional motorized wheelchair and (b) on an industrial motorized cart.

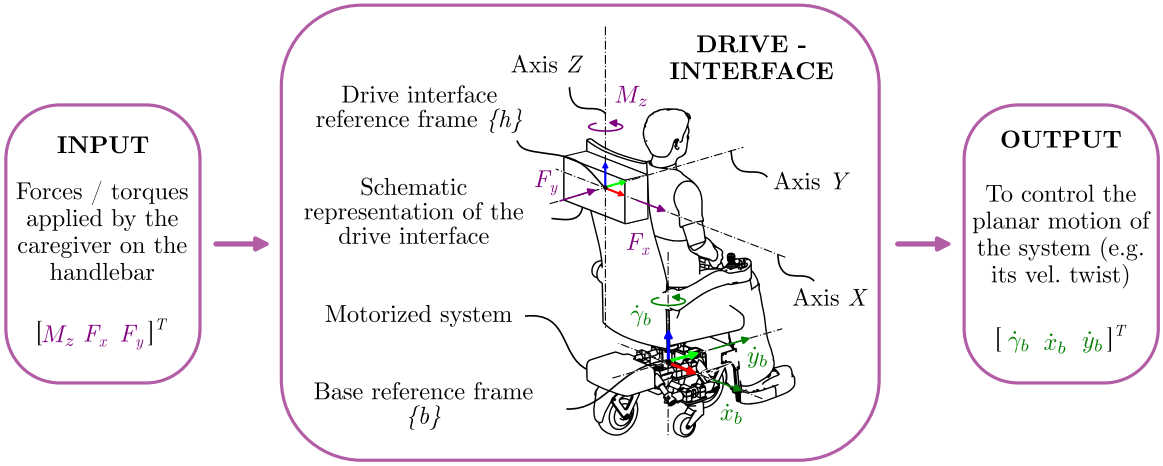

FIGURE 2 | Concept of the drive interface.

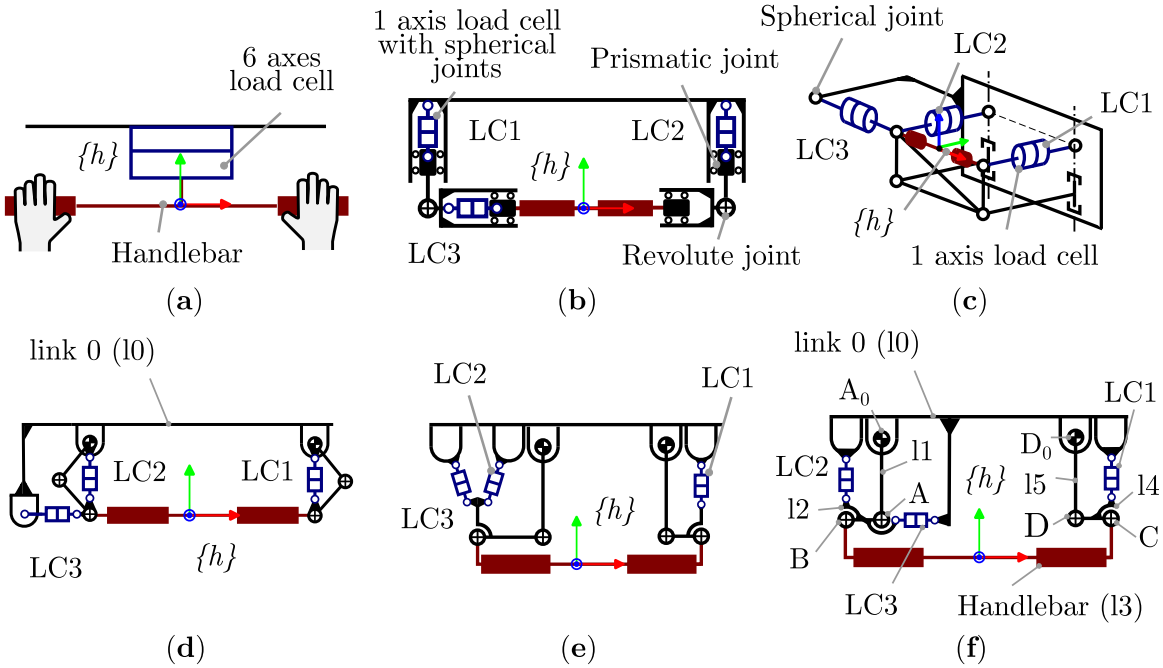

FIGURE 3 | Some of the mechanisms considered during the functional design of the sensorized handlebar: (a) with a six-axis force/torque sensor, (b) a four-bar-like handlebar with four prismatic joints, two revolute joints and three uniaxial load cells, (c) a spatial linkage with two revolute joints, four spherical joints and binary links, (d) a six-bar linkage mechanism, (e) a six-bar linkage with a different load cell arrangements compared with (d), and (f) the six-bar linkage adopted in the final design of the sensorized handlebar.

system through a six-axis force/torque sensor. As mentioned before, this solution is very simple and high-quality measurements can be achieved, based on the quality of the adopted force/torque sensor. These sensors are commonly used in collaborative robotics to measure the forces and torques related to the interaction between the robot end-effector and its environment. Therefore, it is easy to find sensors within the appropriate force/torque range. Unfortunately, six-axis force/torque sensors are very expensive and for this reason this solution is not suited for the device under development. As discussed in Section 1, this study investigates the use of an isostatic structure with only uniaxial load cells to measure the components of interest of the force/torque wrench applied by the driver on the handlebar. Figure 3b–f depicts some of the possible layouts that have been considered during the functional design of the device. In particular, solution (b) adopts three single-axis load cells mounted on a three-degrees-of-freedom planar mechanism made of four prismatic joints and two revolute joints. As a downside, this solution is characterized by high mechanical complexity and its functioning is strongly dependent on friction. Solution (c) uses three uniaxial load cells mounted on a spatial articulated mechanism composed of two revolute joints, four spherical joints, and six binary links. This solution has the same advantages of solution (b) related limited cost associated with single-axis load cells, but it has a high mechanical complexity and higher encumbrance. Solutions (d)–(f) are based on a six-bar linkage. If we consider the structure without the uniaxial load cells, the handlebar can translate in the *XY*-plane and rotate around the *Z*-axis of the *h* frame. Solution (f) is characterized by a particular

configuration of the links if compared with solution (d), and a particular layout of the uniaxial load cells, if compared with solution (e). Due to these characteristics, this solution has a limited lateral encumbrance and can achieve higher measurement accuracy. To better describe how the mechanism configuration enhances the measurements, let us imagine the system without the three load cells (i.e., let us consider the planar six-bar linkage A_0ABCDD_0 in Figure 3f). Because of the mechanism pose, a very small translation of the handlebar along the Y-axis (the revolute joints B and C translate along the Y-axis) implies that the distance variation between the attachment point of LC3 can be considered negligible. Similarly, a small translation of the handlebar along the X-axis (the revolute joints B and C translate along the X-axis) does not change the distances between the attachment points of LC1 and LC2. For this reason, the measurements can be considered decoupled with a consequent lower influence of the assembly precision on the load measurements. Because of these advantages, configuration (f) is selected to be implemented on the wheelchair prototype.

When discussing force-sensitive interfaces, an important aspect to consider is the ability to distinguish whether the measured forces are being applied intentionally by the driver or are the result of accidental impacts. If the forces originate from the driver, they should be used to control the motion of the system; otherwise, they should be disregarded. To detect whether the person is actively holding the SensHB.Q handlebar, numerous strategies, such as dead-man switches, touch sensors, pressure sensors, or image recognition systems, could be used. In this case, the handlebar is provided with capacitive sensors integrated into the ergonomic grips beneath the fingers of the driver, as shown in Figure 4. By monitoring the status of these switches, it is possible to determine whether the driver is gripping the handles or not.

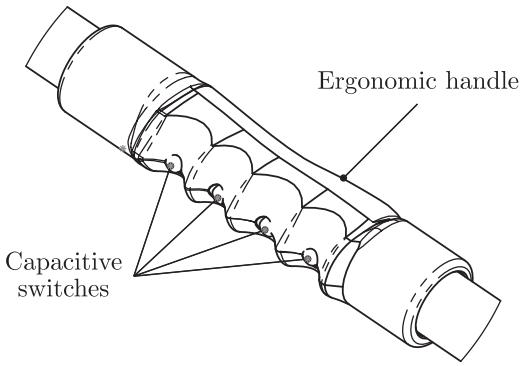

FIGURE 4 | Representation of an ergonomic handle with capacitive sensors placed beneath the fingers of the driver.

4 | SensHB Prototype

This section illustrates the prototype of SensHB that was developed to test the sensorized-handlebar concept. Figure 5 shows a render view of the prototype. Spring steel flexible bands are adopted to create flexure hinges for the mechanism instead of conventional revolute joints, as shown in the details in Figure 5.

Compliant revolute joints are particularly suited for this kind of application. In fact, since the device is an isostatic structure, ideally no range of motion is required and, therefore, both the elastic spring behavior of flexure hinges and the nonlinear deformation of the flexible elements can be neglected. Finally,

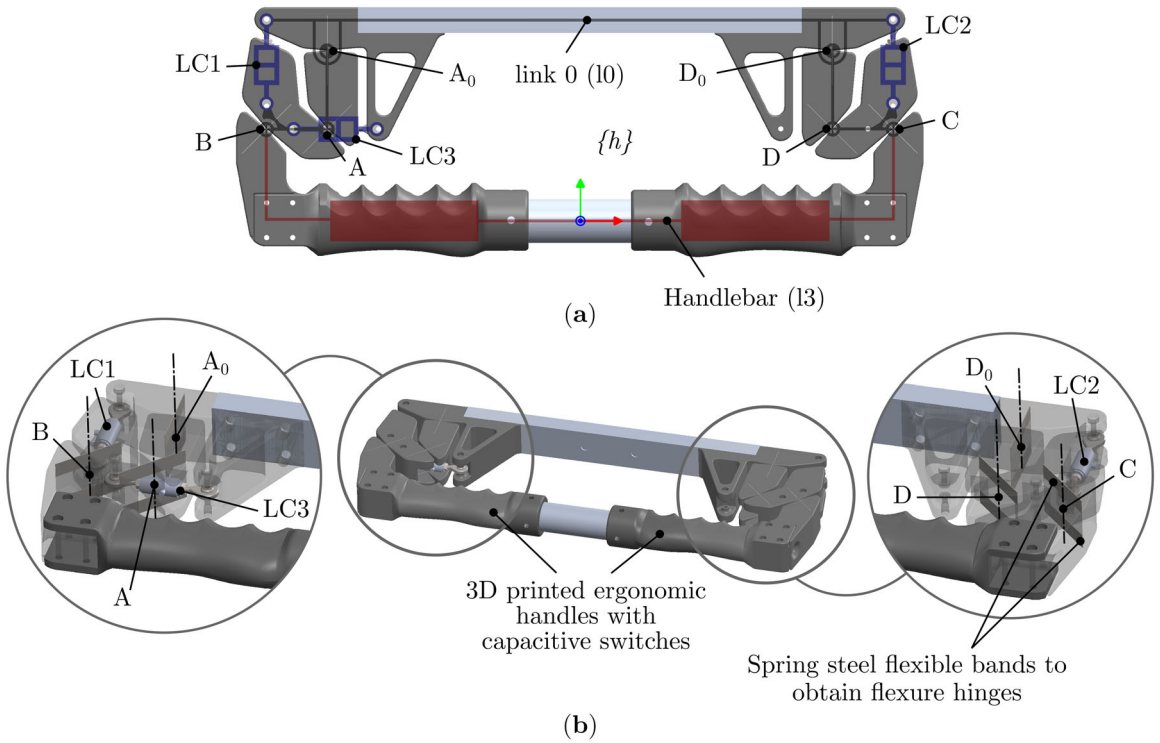

FIGURE 5 | Render view of the executive design of SensHB made of flexure hinges: (a) top view with the functional scheme in transparency and (b) three-dimensional view.

another important advantage related to the adoption of compliant revolute joints is that static friction in the revolute pairs can be eliminated.

The majority of the components are 3D printed except for two elements. The first is an aluminum profile 30 × 15 mm that is used as fixed link that connects the device to the motorized system to be controlled, while the second one is an aluminum tube (25 mm in diameter) that connects the ergonomic handles.

Figure 6 presents the prototype of SensHB. Figure 6 also highlights the three uniaxial load cells and the sensitive parts of the capacitive switches installed inside the ergonomic handles. The adopted load cells, model FLAE-100N, and amplifier, model LC3A(0-2.5-5V)-24V, are produced and calibrated by Forsentek Co. The load range that can be measured is ±100 N and the static gain is 0.050 V/N considering also the amplifier.

5 | Electronic System

Since the sensorized handlebar is conceived to be an independent drive interface, a dedicated control unit is developed. The device needs to output, at least, the following information:

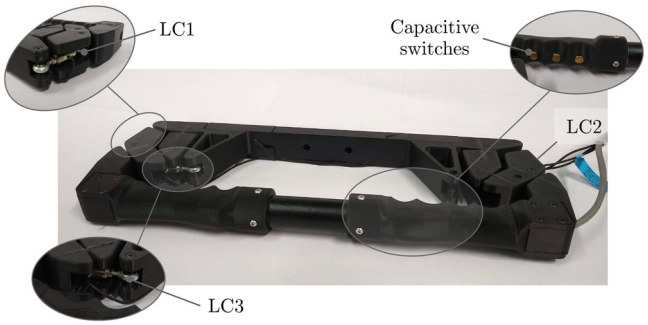

FIGURE 6 | SensHB prototype: Detail of the uniaxial load cells and capacitive switches.

- ON/OFF: A Boolean variable that is true when the sensorized handlebar is powered, and it is false when it is not.
- ENABLED/DISABLED: A Boolean variable that is only true when the driver holds correctly the handlebar.
- OUT1, OUT2, and OUT3: Output variables that are related to the force wrench applied by the driver.

From a functional point of view, the logic implemented on the electronic system can be represented as in Figure 7. The microcontroller reads the state of the capacitive switches (four for each handle). If at least one switch for each handle is active (two switches are active for the one-hand version), then the handlebar is activated. In this state, the amplified load cell signals are red and, then the command references for the system to be controlled (e.g., desired velocity twist) are generated. If the handlebar if off (i.e., it is not properly held) a stop routine is activated using a deceleration ramp that can be customized according to the needs. The core of this control system is the algorithm to generate the command references for the motorized system to be controlled. In Figure 7 this algorithm is referred to as velocity twist generator, since velocity twist commands are widely used to control the motion of mobile systems, such as mobile robots and EPWs. The way force/torque inputs are used to generate motion commands has a strong influence on the user experience. As it is described in Section 7, this study proposes the use of specific map functions to convert the measured driver wrench into velocity commands for the omnidirectional EPW MoviWE.Q.

The electronic control system of the sensorized handlebar is designed around an Arduino UNO Rev4. A specific capacitive sensor, the CAP1188 Capacitive Touch Sensor Breakout from Adafruit, is included to read the status of the capacitive switches. This sensor implements algorithms to estimate the capacity connected to the pins, filters the signals, and performs a calibration routine at start-up. The output signals can be transmitted using serial communication or with analog signals. Finally, the device is powered by an external battery (voltage range from 25.2 to 35 V) that can be the battery of the device to be controlled. The

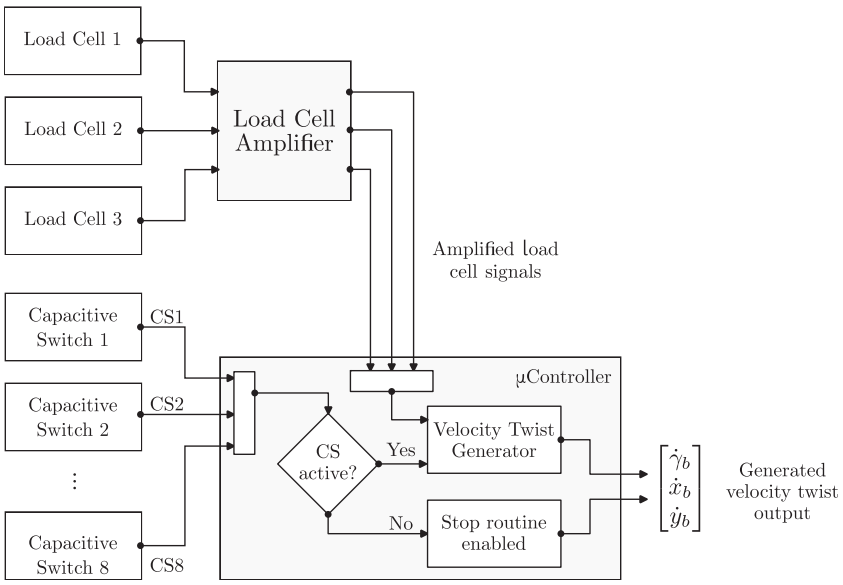

FIGURE 7 | Sensorized-handlebar control system: Schematic representation.

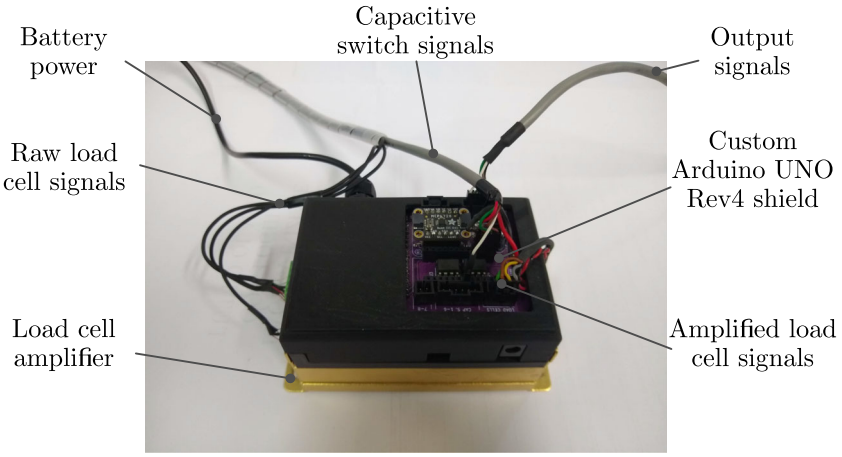

FIGURE 8 | Photo of the electronic system.

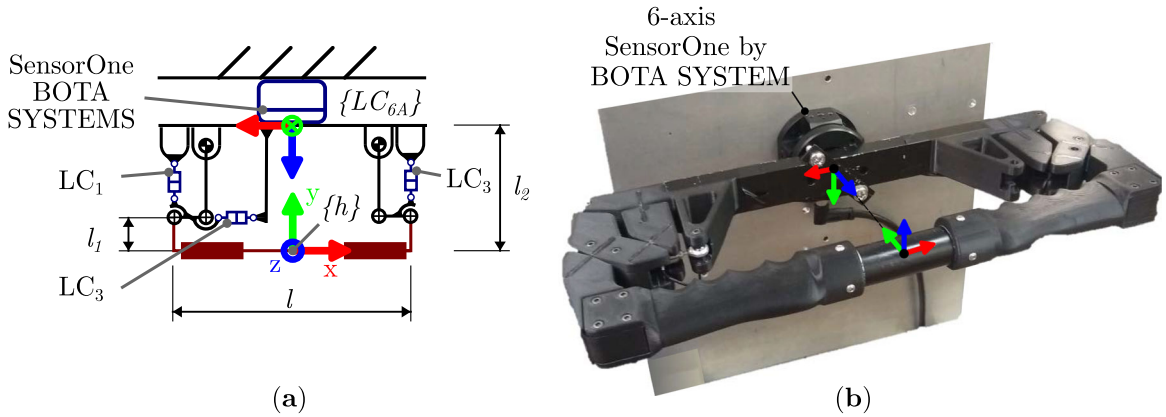

FIGURE 9 | Experimental setup: (a) schematic representation and (b) photo.

electronic control system is shown in Figure 8. A custom printed circuit board was designed and manufactured to integrate all the components.

6 | Experimental Tests

To evaluate the accuracy of prototype, experimental tests in the laboratories of Politecnico di Torino have been conducted. Figure 9 shows the experimental setup adopted to compare the sensorized-handlebar measurements with the ones from a commercial six-axis force/torque sensor, the SensorOne by BOTA SYSTEMS.

The driver applies forces and moments (wrench) on the handlebar that can be described with respect to (wrt) the reference frame (rf) $\{h\}$ as

$$ {}^{h}W_{\text{user}} = {}^{h}[M_x \quad M_y \quad M_z \quad F_x \quad F_y \quad F_z]^T_{\text{user}}. \tag{1} $$

The components M_x, M_y, and F_z are transmitted to the constraining reactions provided by the structure of the device, while the other three components of ${}^{h}W_{\text{user}}$ are measured using the three uniaxial load cells LC_1, LC_2, and LC_3. In particular, the relation between the forces measured by the uniaxial load cells F_{LCi} $(i = 1, 2, 3)$ and the interesting components of the driver wrench is described by Equation (2):

$$ {}^{h}\begin{bmatrix} M_z \\ F_x \\ F_y \end{bmatrix}_{\text{user}} = \begin{bmatrix} \frac{l}{2}(F_{LC1} - F_{LC2}) - l_1 F_{LC3} \\ F_{LC3} \\ F_{LC1} + F_{LC2} \end{bmatrix} = \begin{bmatrix} \frac{l}{2} & -\frac{l}{2} & -l_1 \\ 0 & 0 & 1 \\ 1 & 1 & 0 \end{bmatrix} \begin{bmatrix} F_{LC1} \\ F_{LC2} \\ F_{LC3} \end{bmatrix}. \tag{2} $$

The six-axis force/torque sensor measures the wrench ${}^{LC_{6A}}W_{\text{user}}$. To compare the measurements of the two systems, the reading of the sensorized handlebar are transposed in the rf $\{LC_{6A}\}$ using Equation (3).

$$ {}^{LC_{6A}}W_{\text{user}} = {}^{LC_{6A}}\begin{bmatrix} M_y \\ F_x \\ F_z \end{bmatrix}_{\text{user}} = \begin{bmatrix} -1 & -l_2 & 0 \\ 0 & -1 & 0 \\ 0 & 0 & -1 \end{bmatrix} h \begin{bmatrix} M_z \\ F_x \\ F_y \end{bmatrix}_{\text{user}}. \tag{3} $$

Ten tests were conducted to compare the force/torque measurements coming from the sensorized handlebar and the commercial six-axis force/torque sensor. During each test, the driver applies random forces and torques to the handlebar.

Measurements are acquired at the same time with both systems. The root-mean-square errors of the wrench components F_x, F_z, and M_y wrt $\{LC_{6A}\}$ are reported in Table 1. As an example, the measurements of test number 9 are shown in Figure 10.

While evaluating these results, it is important to consider the final application of the sensorized handlebar, that is, to acquire information from the caregiver about the desired motion of the wheelchair. From this point of view, the measurements look promising to test the functioning of the sensorized handlebar on a practical use case with a mean root-mean-square error of 2.34 N on F_x, 0.85 N on F_z, and 0.14 Nm on M_y. The biggest measured differences are related to the x-component of the force. This difference can be explained with the high noise level of the measurement coming from the commercial six-axis force/torque sensor.

7 | Case Study: Application on the Omnidirectional Wheelchair MoviWE.Q

To evaluate the functionality of the developed prototype, a preliminary experimental test was conducted in the laboratories of Politecnico di Torino, where the sensorized handlebar was mounted on the omnidirectional EPW MoviWE.Q (Tagliavini and Quaglia 2023). MoviWE.Q is designed to overcome the mobility limitations of conventional wheelchairs by enhancing navigation capabilities in indoor environments with obstacles and narrow passages. Omnidirectional mobility is achieved through two independent swerve-drive units, each composed of a motorwheel mounted on a motorized vertical steering axis that intersects the motorwheel's axis of rotation. By controlling these four degrees of freedom, it is possible to manage all three degrees of freedom of MoviWE.Q. Further details about MoviWE.Q are provided in the previous work (Tagliavini and Quaglia 2023).

In this context, the sensorized handlebar serves as an interface for caregivers to drive the omnidirectional EPW, leveraging its high mobility. Figure 11 illustrates the SensHB prototype mounted on MoviWE.Q. Specifically, Figure 11a shows the entire system along with the reference frames of the sensorized handlebar ($\{h\}$) and the wheelchair base (b), while Figure 11b,c provides detailed views of the handlebar prototype.

The caregiver's wrench is measured by the sensorized handlebar with respect to the load cell measurements in the $\{h\}$ frame using Equation (2). These measurements are then transposed

TABLE 1 | Root-mean-square (RMS) errors of the wrench components F_x, F_z, and M_y wrt $\{LC_{6A}\}$ between the force/torque measurements of the sensorized handlebar and the six-axis force sensor.

Test No.	RMS_{F_x} (N)	RMS_{F_z} (N)	RMS_{M_y} (Nm)	Test No.	RMS_{F_x} (N)	RMS_{F_z} (N)	RMS_{M_y} (Nm)
1	2.24	0.75	0.13	6	2.33	0.73	0.14
2	2.46	0.83	0.14	7	2.06	0.80	0.13
3	2.21	0.82	0.15	8	2.66	1.08	0.17
4	2.93	1.10	0.16	9	1.87	0.69	0.12
5	2.72	1.02	0.16	10	1.91	0.68	0.12

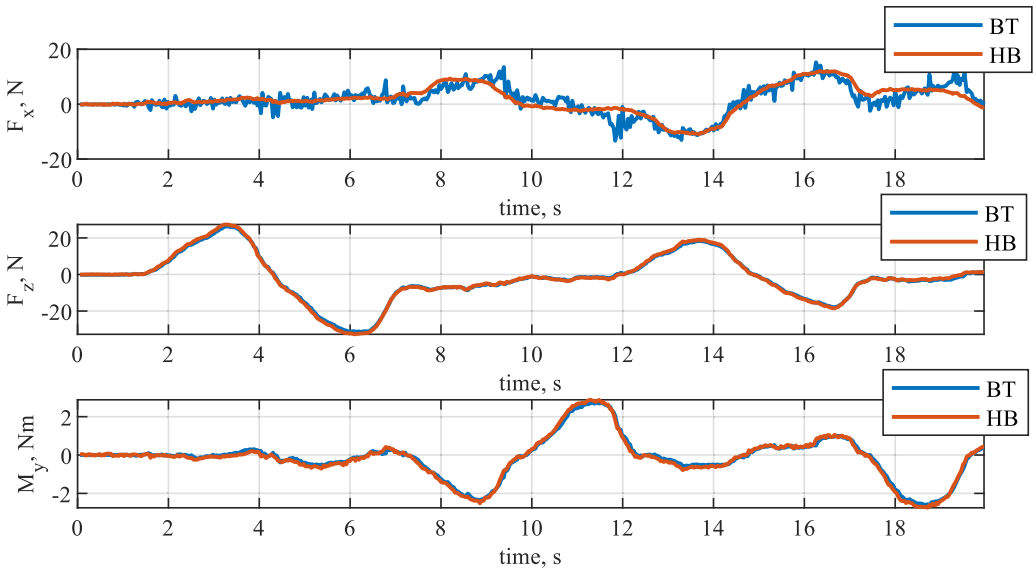

FIGURE 10 | Experimental results: test number 9. The acronym "BT" stands for the six-axis force torque sensor by BOTA SYSTEMS, while "HB" stands for the forces and torque measured with the sensorized handlebar. The wrench components are reported in the $\{LC_{6A}\}$ reference frame.

into the wheelchair base reference frame according to the following relationship:

$$ {}^{b}W_{\text{user}} = {}^{b}\begin{bmatrix} M_z \\ F_x \\ F_y \end{bmatrix}_{\text{user}} = \begin{bmatrix} 1 & l_3 & 0 \\ 0 & 1 & 0 \\ 0 & 0 & 1 \end{bmatrix} h \begin{bmatrix} M_z \\ F_x \\ F_y \end{bmatrix}_{\text{user}} . \quad (4) $$

Given the caregiver wrench expressed in the $\{b\}$ frame, different approaches can be adopted to generate the velocity twist reference for the wheelchair. The method of utilizing force/torque inputs significantly impacts the user experience. In this study, the wrench components are converted into a two-dimensional (2D) velocity twist using specific mapping functions, as depicted in Figure 12. The detailed mathematical description of these mapping functions is beyond the scope of this study, which focuses on the design and testing of the sensorized handlebar. From a functional perspective, the generation of the velocity twist command is illustrated in Figure 13.

Experimental tests are conducted to evaluate the effectiveness of the handlebar in controlling the MoviWE.Q wheelchair. Specifically, the tests are considered successful if the interface allows drivers to control all three degrees of freedom of the

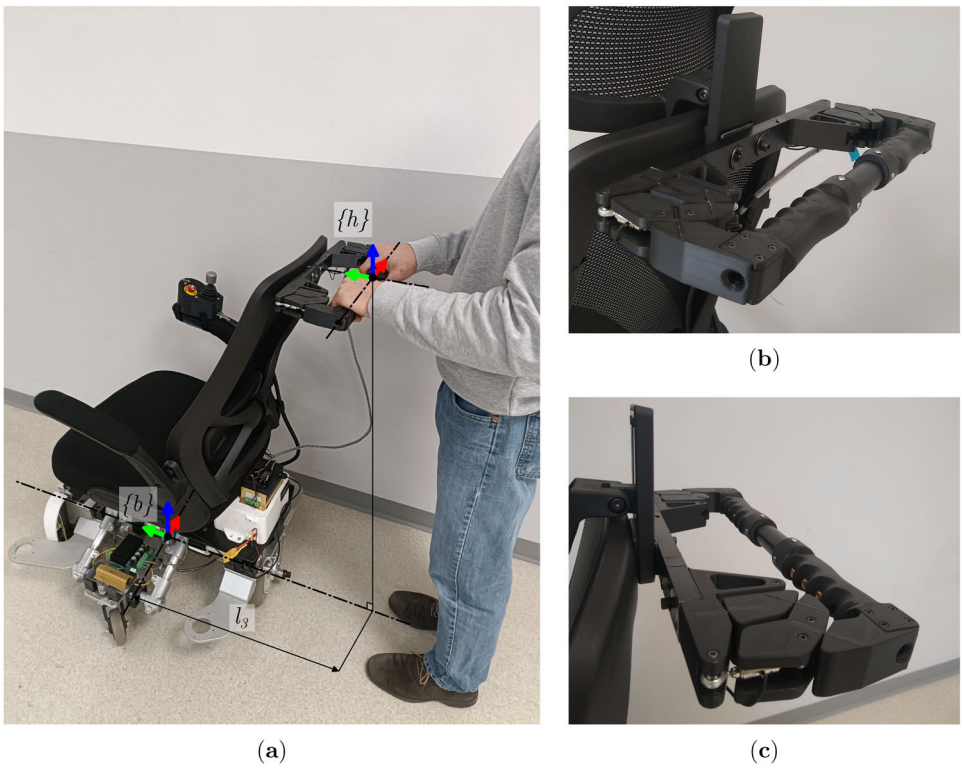

FIGURE 11 | SensHB prototype mounted on the omnidirectional electric-powered wheelchair MoviWE.Q: (a) reference frame definition and (b, c) detail view of the sensorized handlebar.

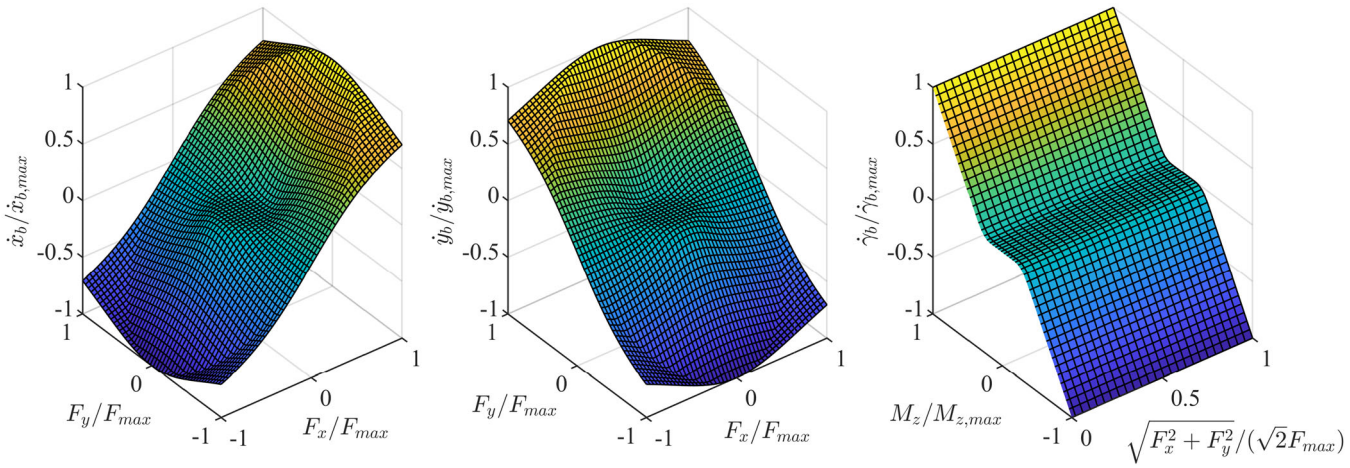

FIGURE 12 | Map functions used to convert the measured caregiver wrench into velocity commands for the omnidirectional wheelchair MoviWE.Q.

wheelchair, if it is easy to use, and if it requires minimal physical effort. Two sets of tests are designed to assess the effectiveness of the sensorized handlebar:

- driving inside a track with obstacles and narrow passages,
- driving on an inclined ramp.

These preliminary tests are conducted with six participants coming from the research group: four men and two women aged 25–61.

7.1 | Test 1: Description and Results

During Test 1, each volunteer is asked to drive the MoviWE.Q wheelchair using the sensorized handlebar from a starting position to a destination, avoiding the obstacles present on the test track, as shown in Figure 14. Various objects are placed along the path to serve as obstacles, testing the navigability through narrow passages.

Each volunteer is asked to keep the wheelchair's orientation steady in the initial part of the track, before reaching the column in the center of the room (red section in Figure 14a). During the tests, the wheelchair's trajectory is recorded using a 2D lidar (Rplidar A2m8 from Slamtec) installed on the wheelchair base, along with the Hector SLAM algorithm (Kohlbrecher et al. 2011) running within the Robot Operating Systems Noetic framework on an Ubuntu 20.04 machine. Additionally, the forces applied to the handlebar and the generated command velocity twist are recorded. Each volunteer has approximately 5 min to drive the system around before data acquisition, allowing them to familiarize themselves with its functioning and the handlebar's sensitivity.

The main goal of these tests was to answer the following question: "Is it possible to drive the omnidirectional EPW MoviWE.Q using the force-sensitive interface SensHB.Q?" While evaluating the functioning of the developed prototype, a preliminary evaluation of the perceived usability of the device was assessed as a secondary outcome.

To assess the intuitiveness and usability of the system, each volunteer completes a questionnaire based on NASA's Raw Task Load Index (NASA-RTLX) (Hart and Staveland 1988; Hart 2006). The subjective workload assessment includes six subscales: Mental Demand, Physical Demand, Temporal Demand, Performance (OP), Effort (EF), and Frustration. Each scale is presented as a line divided into 20 equal intervals, with 21 vertical tick marks dividing the scale from 0 to 100 in

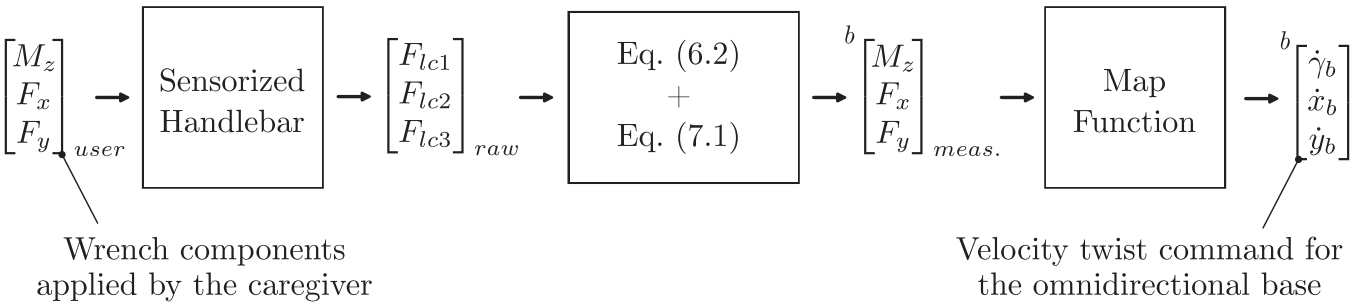

FIGURE 13 | Velocity twist command generation sequence.

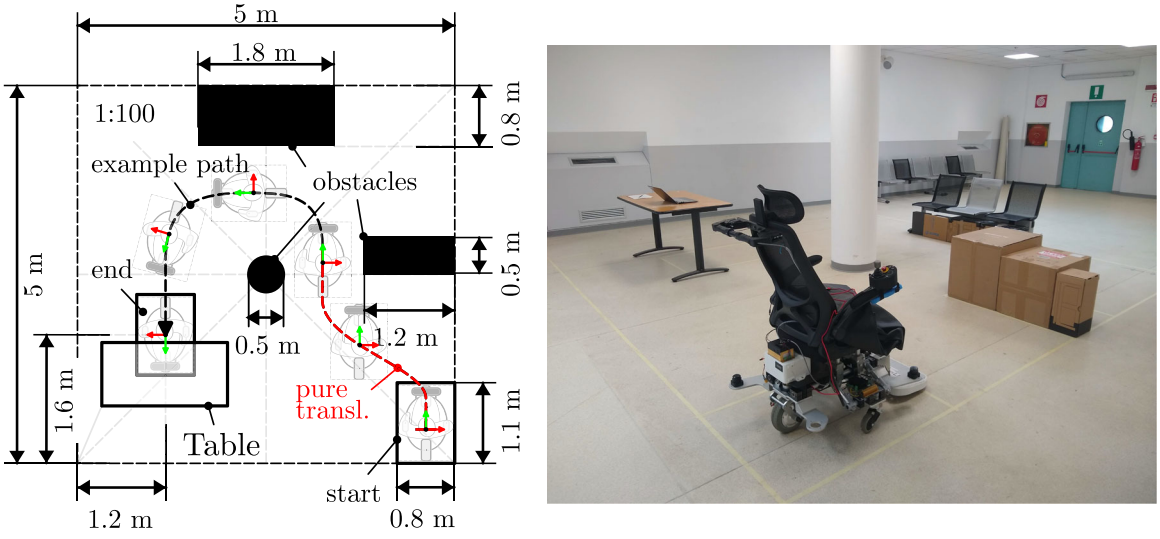

FIGURE 14 | Test track: (a) top view scheme with dimensions and (b) photo of the test track.

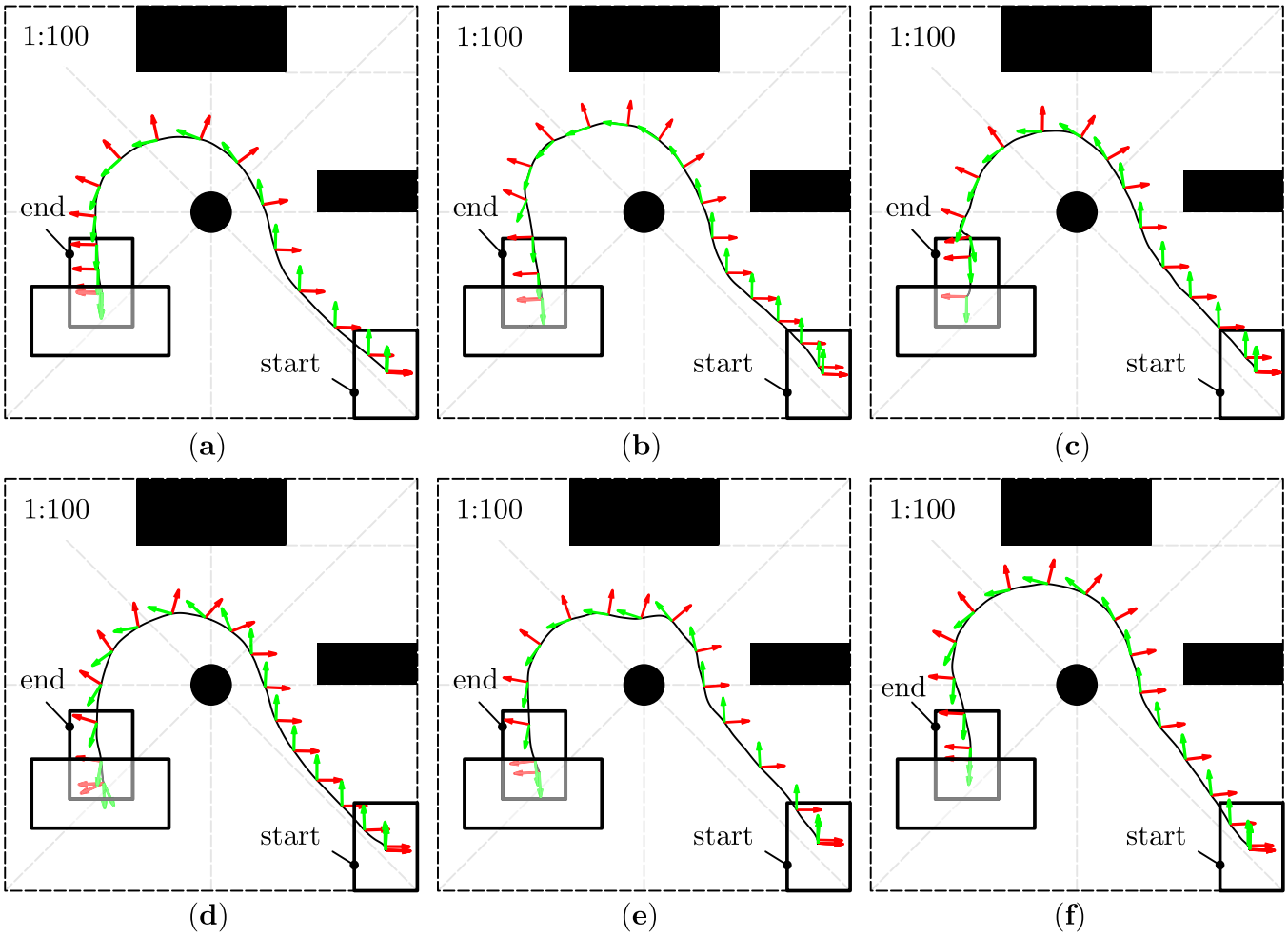

FIGURE 15 | Trajectories of the wheelchair base during the tests: (a) first volunteer, (b) second volunteer, (c) third volunteer, (d) fourth volunteer, (e) fifth volunteer, and (f) sixth volunteer.

TABLE 2 | NASA's RLTX results for the six volunteers over the subscales: Mental Demand (MD), Physical Demand (PD), Temporal Demand (TD), Performance (OP), Effort (EF), and Frustration (FR).

No.	MD	PD	TD	OP	EF	FR	TOT
1	15/100	5/100	10/100	25/100	25/100	10/100	90/600
2	20/100	10/100	15/100	20/100	20/100	15/100	100/600
3	30/100	10/100	10/100	10/100	35/100	15/100	110/600
4	25/100	35/100	35/100	15/100	20/100	20/100	150/600
5	5/100	20/100	5/100	10/100	20/100	5/100	65/600
6	10/100	45/100	20/100	10/100	15/100	20/100	120/600
Average	17.5/100	20.8/100	15.8/100	15/100	22.5/100	14.2/100	105.8/600

increments of 5. The results are considered positive if the workload needed to accomplish the task is low, which corresponds to a low score in the NASA-RTLX's scales.

Figure 15 shows the trajectories of the wheelchair base during the tests for all six volunteers. The results indicate that all participants successfully completed the task, parking the wheelchair under the table. As requested, the drivers maintained a steady orientation in the first part of the path. The drivers accomplished the task in an average time of $T = 31.13$ s (the track length is around 7 m), with individual times as follows: (a) 28.38 s, (b) 35.34 s, (c) 38.81 s, (d) 27.81 s, (e) 25.07 s, and (f) 31.37 s. The same task was performed five times with a person seated in the wheelchair and driving using the three-axis joystick of MoviWE.Q, resulting in an average time of 29.23 s. The comparable average times suggest that drivers were able to complete the task in a reasonable time using the sensorized handlebar.

The results of NASA's RLTX tests are presented in Table 2. In NASA's Raw Task Load Index, the weighting process is omitted,

and the scores are summed to create an estimate of overall workload. Additionally, averages over the individual subscales are computed to estimate the factor's influence on the overall subjective workload. None of the subscales registered an average evaluation above 22.5/100. As noted by Hart Hart (2006), it is challenging to identify a "redline," or a point on the scale that indicates when workload is not only high but excessively high. However, based on the results, the workload associated with the task was generally low. The primary contributor to the total workload appears to be the EF required to achieve the desired OP level.

It is important to highlight the limitations of this usability evaluation. First, the number of volunteers in this study was limited and may not be fully representative of all potential users of the technology. Second, NASA's Raw Task Load Index was adopted to assess perceived workload, but this method has some limitations, such as subjectivity and self-report bias. Therefore, these results should be considered as preliminary positive feedback on the use of the handlebar. In-depth usability tests are beyond the scope of this study but will be addressed in future publications.

7.2 | Test 2: Description and Results

One of the goals of adopting the handlebar is to reduce the physical EF required to operate the motorized system. Ideally, the driver should exert minimal forces and torques on the handlebar, with all traction forces provided by the motorized system. To experimentally validate this feature, four tests are conducted on an inclined ramp. During these tests, the driver is instructed to move the wheelchair along a straight path: five meters on flat ground followed by five meters on a 4° inclined ramp, as illustrated in Figure 16a. The tests are considered successful if the driver can maintain a constant speed while applying the same level of force throughout the tests.

Figure 16b presents the applied force on the handlebar alongside the wheelchair speed in the direction of movement. As depicted in the plots, the driver maintains a consistent force level during both the flat-ground and inclined-ramp sections, resulting in a nearly constant velocity of the wheelchair. This observation suggests that the adoption of the handlebar effectively reduces the physical EF required by the driver.

8 | Conclusion

This study aimed to develop an intuitive control interface, named SensHB, for motorized systems, such as mobile robots, motorized carts, lifts, and wheelchairs. The SensHB device is designed to be cost-effective, featuring an isostatic structure with three uniaxial load cells that constrain a planar mechanism using flexure revolute hinges. A prototype of SensHB was developed and subjected to testing.

Initially, the accuracy of the handlebar measurements was validated by comparing them against readings from a commercial six-axis force/torque sensor, yielding positive results as detailed in Section 6. Subsequently, the paper presented a case study involving the sensorized handlebar mounted on the omnidirectional EPW MoviWE.Q. Two sets of experimental tests were conducted to assess the efficacy of SensHB in controlling the MoviWE.Q wheelchair: navigating through a track with obstacles and narrow passages, and ascending an inclined ramp. It is important to acknowledge that the number of volunteers involved in this study was limited and may not fully represent all potential users of the technology. Nevertheless, the outcomes of these tests provide preliminary positive feedback on the usability of the handlebar. To generalize these findings, future studies involving a larger and more diverse participant group would be beneficial.

In conclusion, the development of SensHB represents a step towards creating an effective and affordable control interface for omnidirectional motorized systems, with promising initial results warranting further investigation and validation.

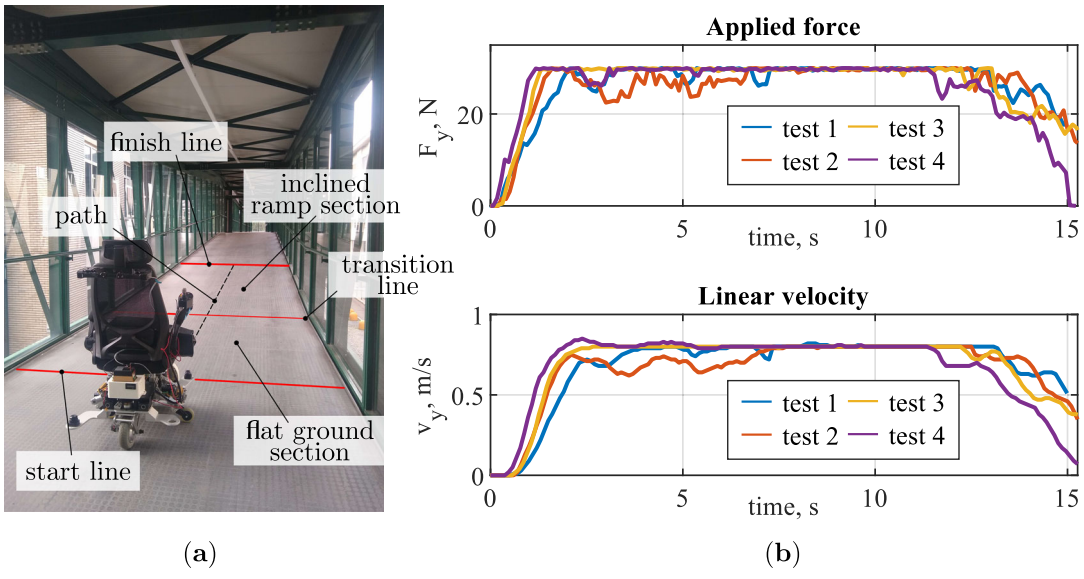

FIGURE 16 | Test 2: (a) experimental setup and (b) results.

Acknowledgments

Open access publishing facilitated by Politecnico di Torino, as part of the Wiley - CRUI-CARE agreement.

Data Availability Statement

The data that support the findings of this study are available from the corresponding author upon reasonable request.

References

Alwan, M., A. Ledoux, G. Wasson, P. Sheth, and C. Huang. 2007. "Basic Walker-Assisted Gait Characteristics Derived From Forces and Moments Exerted on the Walker's Handles: Results on Normal Subjects." *Medical Engineering & Physics* 29, no. 3: 380–389.

Blanchard, F. W., J. J. Thompson, D. J. Wrobleski, and M. S. Smith. 2013. Patient Support Apparatus. US Patent 8,413,271.

Bruzzone, L., and G. Quaglia. 2012. "Locomotion Systems for Ground Mobile Robots in Unstructured Environments." *Mechanical Sciences* 3, no. 2: 49–62.

Choi, J. 2025. "Advanced Omni-Directional Mobility System for Human-Friendly Industrial Warehouse Operations." In *IEEE Transactions on Industry Applications*, Vol. 61, 4364–4372. IEEE.

Choi, J. H., Y. Chung, and S. Oh. 2019. "Motion Control of Joystick Interfaced Electric Wheelchair for Improvement of Safety and Riding Comfort." *Mechatronics* 59: 104–114.

Cortes, U., A. Martínez-Velasco, C. Barrué, et al. 2008. "Towards an Intelligent Service to Elders Mobility Using the i-Walker." In *AAAI Fall Symposium: AI in Eldercare: New Solutions to Old Problems*, 32–38. American Association for Artificial Intelligence.

Ding, D., and R. A. Cooper. 2005. "Electric Powered Wheelchairs." *IEEE Control Systems Magazine* 25, no. 2: 22–34.

Hart, S. G. 2006. "NASA-Task Load Index (NASA-TLX); 20 Years Later." In *Proceedings of the Human Factors and Ergonomics Society Annual Meeting*, Vol. 50, 904–908. Sage Publications.

Hart, S. G., and L. E. Staveland. 1988. "Development of NASA-TLX (Task Load Index): Results of Empirical and Theoretical Research." In *Advances in Psychology*, Vol. 52, 139–183. Elsevier.

Kim, H., and W. Chang. 2022. "Intuitive Drone Control Using Motion Matching Between a Controller and a Drone." *Archives of Design Research* 35, no. 1: 93–112.

Kohlbrecher, S., J. Meyer, O. von Stryk, and U. Klingauf. 2011. "A Flexible and Scalable SLAM System With Full 3D Motion Estimation." In *Proceedings of the IEEE International Symposium on Safety, Security and Rescue Robotics (SSRR)*. IEEE.

Lapointe, J.-F., and N. G. Vinson. 2002. "Effects of Joystick Mapping and Field-of-View on Human Performance in Virtual Walkthroughs." In *Proceedings of the First International Symposium on 3D Data Processing Visualization and Transmission*, 490–493. IEEE.

Marchal, M., J. Pettré, and A. Lécuyer. 2011. "Joyman: A Human-Scale Joystick for Navigating in Virtual Worlds." In *2011 IEEE Symposium on 3D User Interfaces (3DUI)*, 19–26. IEEE.

Martins, M., C. Santos, E. Seabra, A. Frizera, and R. Ceres. 2014. "Design, Implementation and Testing of a New User Interface for a Smart Walker." In *2014 IEEE International Conference on Autonomous Robot Systems and Competitions (ICARSC)*, 217–222.

Murakami, W. 2019. Robot Operating Apparatus Provided With Handles for Operating Robot. US Patent 10,300,608.

Neaz, A., S. Lee, and K. Nam. 2023. "Design and Implementation of an Integrated Control System for Omnidirectional Mobile Robots in Industrial Logistics." *Sensors* 23, no. 6: 3184.

Nosirov, K., S. Begmatov, and M. Arabboev. 2020. "Analog Sensing and Leap Motion Integrated Remote Controller for Search and Rescue Robot System." In *2020 International Conference on Information Science and Communications Technologies (ICISCT)*, 1–5. IEEE.

Shi, F., Q. Cao, C. Leng, and H. Tan. 2010. "Based on Force Sensing-Controlled Human–Machine Interaction System for Walking Assistant Robot." In *2010 8th World Congress on Intelligent Control and Automation*, 6528–6533. IEEE.

Shibata, M., C. Zhang, T. Ishimatsu, et al. 2015. "Improvement of a Joystick Controller for Electric Wheelchair User." *Modern Mechanical Engineering* 5, no. 4: 132.

Tagliavini, L., G. Colucci, A. Botta, P. Cavallone, L. Baglieri, and G. Quaglia. 2022. "Wheeled Mobile Robots: State of the Art Overview and Kinematic Comparison Among Three Omnidirectional Locomotion Strategies." *Journal of Intelligent & Robotic Systems* 106, no. 3: 57.

Tagliavini, L., and G. Quaglia. 2023. "On the Design of moviwe.q: An Omnidirectional Electric-Powered Wheelchair for Indoor Mobility." In *IFToMM World Congress on Mechanism and Machine Science*, 311–321. Springer.

Taheri, H., and C. X. Zhao. 2020. "Omnidirectional Mobile Robots, Mechanisms and Navigation Approaches." *Mechanism and Machine Theory* 153: 103958.

Trujillo-León, A., W. Bachta, J. Castellanos-Ramos, and F. Vidal-Verdú. 2018. "Assistive Handlebar Based on Tactile Sensors: Control Inputs and Human Factors." *Sensors* 18, no. 8: 2471.

Trujillo-León, A., F. Vidal-Verdú, and W. Bachta. 2017. "Evaluation of Tactile Sensors as an Alternative to Force Sensors in an Assistive Haptic Handlebar." In *2017 IEEE Biomedical Circuits and Systems Conference (BioCAS)*, 1–4. IEEE.

Yang, S., S. Wang, and S. Huang. 2023. "ROS-Based Remote Control of Industrial Robot Joystick." *Proceedings of the Institution of Mechanical Engineers, Part C: Journal of Mechanical Engineering Science* 237, no. 1: 160–169.

Supporting Information

Additional supporting information can be found online in the Supporting Information section.
HandlebarVideo.